An Automated Dental Lesion Detection System Based on Deep Learning

By

Anum Fatima

00000317839

Supervisor

Assoc Prof Dr. Hammad Afzal

Department of Computer Software Engineering

A thesis submitted in partial fulfillment of the requirements for the degree of Masters in Software Engineering (MS SE)

In

School of Electrical Engineering & Computer Science (SEECS) ,

National University of Sciences and Technology (NUST),

Islamabad, Pakistan.

(October 2022)

Thesis Acceptance Certificate

Certified that final copy of MS/MPhil thesis entitled "**An Automated Dental Lesion Detection System Based on Deep Learning**" written by **Anum Fatima**, (Registration No **00000317839**), of Military College of Signals (MCS) has been vetted by the undersigned, found complete in all respects as per NUST Statutes/Regulations, is free of plagiarism, errors and mistakes and is accepted as partial fulfillment for award of MS/M Phil degree. It is further certified that necessary amendments as pointed out by GEC members of the scholar have also been incorporated in the said thesis.

Signature: _____

Name of Advisor: **Assoc Prof Dr. Hammad Afzal**

Date: _____

Signature (HoD): _____

Date: _____

Signature (Dean/Principal): _____

Date: _____

Approval

It is certified that the contents and form of the thesis entitled "**An Automated Dental Lesion Detection System Based on Deep Learning**" submitted by **Anum Fatima** have been found satisfactory for the requirement of the degree.

Advisor: **Assoc Prof Dr. Hammad Afzal**

Signature: _____

Date: _____

Co-Advisor: **Dr. Imran Shafi**

Signature: _____

Date: _____

Committee Member 2: **Lt. Col. Khawir Mahmood**

Signature: _____

Date: _____

Committee Member 3: **Dr. Naima Altaf**

Signature: _____

Date: _____

Dedication

This thesis is wholeheartedly dedicated to my beloved parents and my siblings; particularly my sister without whose constant support, this thesis paper was not possible.

Certificate of Originality

I hereby declare that this submission is my own work and to the best of my knowledge it contains no materials previously published or written by another person, nor material which to a substantial extent has been accepted for the award of any degree or diploma at Department of Computer Software Engineering at Military College of Signals (MCS) or at any other educational institute, except where due acknowledgement has been made in the thesis. Any contribution made to the research by others, with whom I have worked at Military College of Signals (MCS) or elsewhere, is explicitly acknowledged in the thesis. I also declare that the intellectual content of this thesis is the product of my own work, except for the assistance from others in the project's design and conception or in style, presentation and linguistics which has been acknowledged.

Author Name: **Anum Fatima**

Signature: _____

Acknowledgments

In the name of Allah, the Most Gracious, the Most Merciful. All praises belong to Allah, the Lord of the worlds and prayers and peace be upon Muhammad His servant messenger.

First and Foremost, I would like to praise Allah Almighty who has showered countless blessing, knowledge, and opportunities on me. This work would have never become truth, without His guidance. I owe deep gratitude to this university for giving me an opportunity to complete this work. I am extremely grateful to my supervisor Dr. Hammad Afzal and co-supervisor Dr. Imran Shafi for their invaluable advice and continuous support. Their immense knowledge and plentiful experience have encouraged me during phases of research. I highly appreciate the efforts expended by Lt. Col. Khawir Mahmood and Dr. Naima Altaf.

I would like to take this opportunity to say warm thanks to my family for their generous support throughout my life and particularly through the process of pursuing this degree. Last, but not the least, deepest thanks go to all the people who tool part in making this thesis real.

Anum Fatima

Contents

List of Figures

List of Tables

Abstract

Artificial intelligence (AI) has made substantial progress in medicine. Automated dental imaging interpretation is one of the most prolific areas of research using AI. X-ray imaging systems have enabled dental clinicians to identify dental diseases since the 1950s. However, the manual process of dental disease assessment is tedious and error-prone when diagnosed by inexperienced dentists. Thus, researchers have employed different advanced computer vision techniques, machine and deep learning models for dental disease diagnoses using x-ray imagery. Despite the notable development of AI in dentistry, certain factors affect the performance of the proposed approaches. Hence, it is of utmost importance for the research community to formulate suitable approaches, considering the existing challenges and leveraging findings from the existing studies. In this regard, lightweight Mask-RCNN model is proposed for periapical disease detection. The proposed model is constructed in two parts: a lightweight modified MobileNet-v2 backbone and region based network (RPN) is proposed for periapical disease localization on small dataset. To measure the effectiveness of the proposed model, lightweight Mask-RCNN is evaluated on a custom annotated dataset comprising images of five different types of periapical lesions. The results indicate that the proposed model was able to detect and localize periapical lesions with an overall accuracy of 94%, mean average precision (mAP) of 85% and mIoU of 71.0%. The proposed model improves the detection, classification, and localization accuracy significantly using smaller number of images compared to existing methods.

Keywords **-** Disease Detection and segmentation, lightweight deep learning, Mask-RCNN, Periodontal disease

Chapter 1

Introduction and Motivation

1.1 Overview

Artificial intelligence (AI) has been widely forecasted in the field of medicine since its conception over 60 years ago [2, 3, 4, 6]. Although the maturity of AI in the field of dentistry has fallen short in sub-fields such as periodontology, endodontics, orthodontics, restorative dentistry, and oral pathology, keen interest has been witnessed in the past few years as artificial intelligence has become incessantly accessible to researchers. Artificial intelligence has made substantial progress in the diverse disciplines of dentistry including dental disease diagnosis [36], localization [12], classification [47], estimation [50], and assessment of dental disease [8].

On a broader level, AI enables the creation of intelligent machines that can achieve tasks without requiring human intervention. Machine learning (ML) [32] is a subset of AI that utilizes computational algorithms to analyze datasets to make predictions without the need for explicit instructions. Towards a more sophisticated and increasingly independent approach for diagnosis, treatment planning, and risk assessment, there has been seen a profound inclination toward deep learning (DL) applications [23, 29].

1.2 Motivation

Over the past decade, Artificial intelligence has remarkably contributed to the various subdisciplines falling under the category of dentistry, specifically periodontology. Different studies have explored dental disease detection, localization, classification, and

Table 1.1: Strengths and weaknesses of baseline dental lesion localization models

Author, Year (Ref)	Image Modality	Task	Method	Strengths	Weaknesses
Jader et al., 2018 [24]	Panoramic images	Localize missing teeth	M-RCNN with ResNet-101 backbone	The model is helpful in identifying missing or broken teeth with an accuracy of 98%.	- Highly variable data - Other metrics i.e., mAP, IoU are not reported for comparison
Anantharaman et al., 2018 [20]	Colored images	Detect and segment cold/canker sores	M-RCNN with ResNet-101 backbone	The model is helpful in performing pixel-wise segmentation of visible light images of oral cavity with accuracy of 74.4%	- Sparse dataset - Other metrics i.e, mAP, IoU, precision, F1-score, recall are not reported for comparison
Moutselos et al., 2019 [38]	Colored images	Localize and classify caries occlusal surfaces	M-RCNN with FCN and ResNet-101 backbone	The model provided encouraging performance for automatically selecting image texture features and detect lesions without additional pre-processing actions	- The computational complexity is not reported
Chen et al., 2019 [33]	Periapical radiographs	Teeth localization and numbering	Faster-RCNN	The model detects and numbers teeth with recall and precision exceeding 90% on manually annotated dataset	- The model suffers in numbering teeth in complicated cases such as heavily decayed teeth
Laishram & Thongam, 2020 [43]	Panoramic radiographs	Localize and classify different type of teeth	Faster-RCNN built on RPN and ODN	The model is helpful in detecting different types of teeth achieving mean average precision (mAP) of 91.40% and accuracy of 91.03%	- Limited dataset in terms of size
Zhu et al., 2022 [63]	Periapical radiographs	Detection of carious teeth	Faster-RCNN with pretrained ResNet-50	The model is helpful in with an average precision of 73.49%, F1-score of 0.68 with sample detection speed of 0.1923	- It suffers from computational compexity - The model does not identify caries type
Rashid et al., 2022 [61]	Mixed images (colored and periapical radiographic images)	Detect and localize dental carious regions	Hybrid M-RCNN	The model was helpful in localizing dental carious regions with a precision of 81.02% and accuracy of 95.75%	- Limited dataset in terms of size - The model does not identify caries type for both colored and x-ray image

segmentation using different imaging modalities within the dental domain. However, few studies explored dental disease localization as discussed in the literature review. To localize dental carious regions, various challenges are observed in the recent studies, which are discussed in Table 1.1. Further exploration is required to propose detection and localization approaches for dental caries diagnosis in real time.

Faster-RCNN, which extends Fast-RCNN is utilized to localize and number teeth, the model achieves recall and precision of above 90%, however, the model suffers in numbering teeth in complicated cases [33]. Faster-RCN built on region proposal network (RPN) and object detection network (ODN) [43] was able to detect different types of teeth achieving mean average precision (mAP) of 91.40% and accuracy of 91.03%, however, the model was applied on a small dataset. Another variant of Faster-RCNN pretrained on ResNet-50 [63] was employed for the detection of carious teeth, achieving a precision of 73.49%, F1-score of 0.68, however, the model does not identify the type of caries and only localizes caries region.

M-RCNN, which extends Faster-RCNN with pretrained ResNet-101 [24] was found to

be helpful in the identification of missing or broken teeth achieving an accuracy of 98%. However, segmentation performance metrics were not reported. For pixel-wise segmentation of visible light images for identification of oral cavities [20], M-RCNN achieves an accuracy of 74.4%, however, the dataset is sparse and other relevant performance metrics have not been reported for comparison. In another attempt, M-RCNN with a fully convolutional network (FCN) and a backbone of ResNet-101 [38] was investigated to localize occlusal surface caries on a limited dataset and the computational complexity was not reported. In a recent attempt, hybrid M-RCNN [61] was employed to identify dentinal caries on mixed images achieving an average precision of 81.02% and accuracy of 95.75%, however, the model does not identify caries type for both colored and x-ray images. Additionally, M-RCNN with ResNet as backbone requires a substantial amount of calculations to learn and analyze, and the training process for M-RCNN requires high-performance computational resources such as GPU and memory [60]. Further research is required to explore and investigate efficient models for the identification and diagnosis of dental caries.

1.3 Scope

Dental disease detection is a tedious process and requires assistance of dental experts, dentists, orthodonotists, and radiologists in properly diagnosing dental caries and other related disease. The process of manually identifying disease is time consuming and prone to human error. Additionally, due to prevalence of COVID-19, manual dental disease diagnosis is suffering due to lack of physical accessibility of patients for routine checkups. Thus, there is a need for research for robust and accurate dental lesion diagnosis systems to automate the process and provide assistance to dental clinicians in a more efficient and effective manner.

The aim of this research is to persuade researchers to broaden the scope of dental disease diagnosis by proposing a deep learning based system that can be employed by dental clinicians in day-to-day practice for dental disease detection. The main focus of this study is to propose a system able to detect and localize dental lesions to assist dentists in making decisions and plan treatment to prevent or cure lesions at early stages.

1.4 Problem Statement

Visual examination of intraoral radiographs is preferred for dental caries detection, however this process is time consuming and leads to errors due to human intervention. To automate the process of dental diagnosis, different studies explored use of Artificial intelligence. Several deep learning based methods are introduced for disease detection, classification, and segmentation. However, a very few attempts are made for dental disease localization on intraoral radiographs. Additionally, the proposed models for dental disease localization are computing resource intensive and require larger datasets to train and make accurate predictions.

1.5 Key Contribution

The literature review indicates that there is still room for research on the localization and segmentation of caries using periapical radiographic images. There are very few studies focusing on usable carious region detection and localization on periapical radiographs. The existing approaches for dental lesion localization provide the key knowledge which can be adopted by researchers to focus on implementing improved segmentation and localization approaches for dental caries. In this regard, this study makes the following contributions:

- Put forward an automated deep learning based dental caries localization and segmentation model to identify the type of periapical lesion and localize the lesion on periapical radiographs.
- Propose a lightweight MobileNet-v2 with additional layers to enhance the performance of Mask-RCNN on small periapical dataset.
- Preprocess low resolution images to obtain better disease diagnosis performance.
- Comprehensive evaluation and comparison of state-of-the-art deep learning based segmentation and localization methods with proposed model.
- Considering the limitation of data availability, this study introduces an annotated dental lesion dataset to identify periapical lesions.

1.6 Thesis Breakdown

The research has been conducted in different phases and are divided into following chapters:

Chapter 1 Introduction: An overview of already proposed approaches for dental caries detection, scope of research, problem statement and key contributions made.

Chapter 2 Literature Review: Discussion related to already proposed approaches for dental caries detection based on machine and deep learning and proposed clinical decision support systems.

Chapter 3 Design and Methodology: Details of the detection and localization model proposed to diagnose periapical lesions.

Chapter 4 Implementation and Results: Brief explanation of implementation steps and performance evaluation of the proposed model.

Chapter 5 Discussion: An overview of results obtained by the proposed model and limitations of the presented work.

Chapter 6 Conclusion: Conclude the presented work and discuss the impact of the proposed model on detection and localization of dental lesions, and provide future directions.

1.7 Summary

In this chapter, the use of Artificial intelligence in the field of dentistry is discussed along with discussion related to several research studies exploring the use of AI in disease detection, localization, classification, and segmentation. This chapter provides brief overview of the strengths and weaknesses of different studies that employed deep learning based model for disease detection localization indicating the need for further research to explore and investigate efficient models for the identification and diagnosis of dental caries. In addition, this chapter highlights the key contributions of the conducted research to enhance the dental disease diagnosis process.

Chapter 2

Literature Review

2.1 Introduction

Recent advancements in artificial intelligence have contributed significantly to help dental clinicians in making more accurate predictions in an efficient manner. The clinical practices have involved different machine and deep learning approaches for dental lesion diagnosis. Several approaches have been proposed to localize dental lesions and researchers have proposed different localization tools to detect lesions in real-time. The performance comparison of different techniques proposed in periodontology are presented in Table. 2.1 and 2.2. The different machine learning, deep learning approaches along with clinical support decision systems are discussed in the following sections.

2.2 Clinical Support Decision Systems

AI application technology is progressing remarkably in the field of dentistry. Clinical decision support systems to provide expert support to a health practitioner is one example [27]. Moreover, these systems have the capability of solving problems that are too complex to be solved by using conventional methods [19]. Moreover, CDSS provides valuable information to dental practitioners that aids in producing faster and superior dental health outcomes.

In dentistry, the interpretation of data and carrying out proper diagnosis is crucial. However, medical decision-making is cumbersome for doctors in a time-compressed environment. Thus, an intelligent tool is required to assist doctors in making accurate

decisions. These systems come under the category of clinical support decision systems (CDSS). Artificial neural networks (ANNs) have been used as CDSS for diagnosis, classification, and assessment. Several ANN architectures have been employed to assist doctors in making accurate decisions in periodontology. Recently, Geetha et al. proposed a back propagation neural network for tooth decay detection. The model achieved an accuracy of 97.1% and a false positive rate of 2.8% using intraoral radiographs. The study indicates that ANNs can be employed for precise decay detection compared to traditional dental examination methods [42]. Papantonopoulos et al. evaluated multilayer perceptron ANN for bone loss assessment on medical health records. The model provided effective periodontitis classification with an accuracy of 98.1% [10]. Using 230 textual subjects, Shankarapillai et al. proposed a multilayer feed-forward propagation network for effective periodontitis risk prediction [8].

2.3 Machine Learning Approaches

Machine learning (ML) is the scientific study of algorithms and statistical models [32] used for a vast array of processing tasks without requiring prior knowledge or handcrafted rules. Recent years have witnessed the wide spread of ML due to their superior performance for various healthcare applications such as dentistry. ML algorithms fall into two learning types: supervised and unsupervised.

The amount of data generated by healthcare service providers is huge, making the data analysis process cumbersome. ML helps in effectively analyzing the data and gaining actionable insights. Additionally, different dentistry applications can benefit from ML techniques, including disease diagnosis, prognosis, treatment, and automating the clinical workflow. Moreover, ML for clinical applications has great potential to transform traditional healthcare service delivery [22].

To classify enamel, dentin, and pulp caries, Oprea et al. proposed rule-based classification. The authors were able to categorize regions as dentin caries sized over 2mm [5]. Another rule based approach based on gradient histogram and the threshold was proposed by ALbahbah and fellow authors on panoramic radiographs to extract and segment decayed and normal teeth. [14]. For localization of alveolar bone loss, Lin et al. evaluated a level segmentation method based on SVM, KNN, and Bayesian classifier. The model was able to localize alveolar bone loss with high classification effectiveness

[12]. A cluster-based segmentation technique was proposed by Datta and Chaki to detect dental cavities. The proposed model utilized Wiener filter to extract caries lesions followed by region segmentation to monitor the lesion size and growth [11]. To detect and classify proximal carious and non-carious lesions on panoramic radiographs, Na'am et al. explored multiple morphological gradient based image processing method on images with manually cropped regions [17]. An extreme machine learning method based on contrast limited adaptive histogram and gray-level covariance matrix was evaluated by Li and fellow authors, using digital photographs, the model provided an accuracy of 74% for gingivitis identification using a small dataset [37]. To minimize error in diagnosis, authors have proposed methods involving machine learning techniques. Li et al. proposed a plaque segmentation method based on CNN using oral endoscopic images. The results provided performance superior to that of dentists with an accuracy of 86.42% [58].

2.4 Deep Learning Approaches

Recent years have seen a surge of interest in deep learning (DL), a subfield of machine learning (ML), as it allows machines to mimic human intelligence in increasingly independent and sophisticated ways [23, 29]. DL uses multiple layers of non-linear units to analyze and extract useful knowledge from huge amounts of data. The extracted knowledge is then used to produce state-of-the-art prediction results. The neural network architectures used in DL provide the capability to perform automatic and accurate detection in healthcare. Based on the study, DL has enormous potential to bring genuinely impactful applications to the field of dentistry.

Different deep learning approaches have been employed by researchers to pave way for more efficient and effective methods to diagnose dental caries. To classify carious and non-carious teeth on a small labeled dataset, a pretrained convolutional neural network (CNN) was utilized by Prajapati et al. The model was able to classify dental caries, periodontitis, and periapical infection [18]. Lee et al. utilized Deep CNN to diagnose and classify caries using 3000 periapical radiographs. The model achieved an AUC of 0.91 for premolar, 0.89 for molar, and 0.84 for both premolar and molar models [26]. For identification of dental caries, Cantu et al. investigated U-Net on bitewing radiographs. It was found that segmentation based models possess the potential to

aid dental clinicians in detecting and locating dental caries more efficiently [41]. For identification of endo-perio lesions on periapical radiographs, Sajjad et al. investigated AlexNet, the model achieved an accuracy of 98% [39]. For early identification of dental caries, Kumari et al. preprocessed bitewing radiographic images using contrast limited adaptive histogram equalization (CLAHE) and noise filtering followed by meta-heuristic based ResneXt RNN [56].

Deep learning-based methods have gained immense popularity in recent years. Several authors have evaluated methods for bone loss detection in intraoral radiographs, Kim et al. suggested using transfer learning to improve the performance of bone loss and odontogenic cyst lesion detection using panoramic radiographs. The model was useful in tooth numbering with performance superior to that of dental clinicians [35]. Another model using deep-feed forward CNN was evaluated by Krois and fellow authors using panoramic radiographs. The model showed discrimination ability similar to that of three examiners [36]. Duong et al. proposed a U-Net-based network for alveolar bone delineation using high-frequency ultrasound images yielding performance higher than three experts [34]. For the classification of regions on the basis of periodontal bone destruction, Moran et al. demonstrated a ResNet model achieving an accuracy of 82% using 467 periapical radiographs [47]. Using ResNet34 as an encoder with U-Net, Nguyen et al. assessed 1,100 intraoral images for alveolar bone segmentation, the model was able to identify alveolar bone with a dice coefficient of 85.3% [48]. To automate the process of detecting bone lesions and detecting correct shapes, Khan et al. presented a disease segmentation method based on U-Net architecture. The model was able to detect the presence and shape of caries with performance higher than three experts [52]. Another anatomically constrained dense U-Net method was proposed by Zheng et al. for bone lesion identification. Using CBCT images, the model was able to detect the correct shape of the bone and lesion [50]. For periodontitis detection, Li et al. utilized Mask R-CNN with a novel calibration method, using panoramic radiographs, the model diagnosed the severity degree of periodontitis with an accuracy of 82% outperforming that of a junior dentist [46]. In a recent attempt, Lee et al. proposed a VGG-based neural network for diagnosing periodontal bone loss using 1,740 periapical radiographs. The model achieves an accuracy of 99% and AUC of 98% outperforming the performance of three dentists [57].

Radiological examinations help dental clinicians in the identification of teeth abnor-

malities, cysts, infections, cysts, and infections. However, manual examinations are time-consuming and rely solely on a specialist's opinion which may bring differences in the diagnosis. Different methods have been employed by researchers in recent years mainly relying on boundary-based, region-based [45] and threshold-based methods [12], cluster-based. As a first step, Jader et al. employed RCNN for the segmentation of caries and the detection of missing teeth on buccal images. The results indicated that deep learning-based instance segmentation has the potential to automate the process of caries detection and medical report generation [24]. In another attempt to automate the separation of each individual tooth, Laishram and Thongam employed Faster-RCNN. The model was able to detect and classify different types of teeth such as molar, premolar, canine, viz., and incisors [43]. To detect and classify dental caries on occlusal surfaces using colored, Moustselos et al. investigated Mask-RCNN, which extends Faster-RCNN [38]. Anantharaman et al. explored Mask-RCNN on colored images to segment canker and cold sores. The model achieved a pixel accuracy of 74% [20]. To detect the position of teeth on manually annotated periapical radiographs based on prior domain knowledge, Chen et al. utilized Faster-RCNN. It was found that the model can detect teeth position with both precision and recall of above 90% [33]. Recently, Zhu and fellow authors investigated Faster-RCNN to predict the number and locations of dental caries on 200 dental periapical radiographs. The model achieved a mean average precision of 73.49%, an F1-score of 0.68. However, the model does not specify the type of caries identified [63]. A hybrid M-RCNN model was proposed by Rashid et al. capable of detecting and localizing dental lesions on mixed images including both colored and x-ray images. The model achieves a precision of 95.5% for colored images, 84.45% for radiographs, and 81.02%for mixed images [61].

Table 2.1: Summary of related studies for AI application for disease diagnosis in periodontology

AI Application	Author, Year (Ref)	Architecture	Data Modality	Dataset Size Split (Train/ Val/Test or Train/ Test)	Study Factor	Results (Performance metrics/values)	Conclusion
Disease Segmentation	Li et al., 2022 [58]	CNN	Oral endoscope images	607 images Train:320 images Test:287 images 320 / 287	Plaque segmentation	Acc: 0.864 IoU: 0.859	The model is helpful in plaque segmentation on small dataset
Disease Diagnosis	Li et al., 2019 [37]	A method based on contrast limited adaptive histogram (CLAHE), gray-level co-occurrence matrix (GLCM), and extreme machine learning	Digital photographs	93 images Train: 73 images Test: 20 images 73 / 20	Gingivitis identification	Accuracy: 0.74 Sensitivity: 0.75 Specificity: 0.73 Precision: 0.74	The method is helpful for gingivitis identification
Disease Localization	Lin et al., 2015 [12]	Level segmentation based on Bayesian or KNN or SVM classifier	Periapical Radiographs	31 images	Alveolar bone loss	Mean SD True Positive Fraction (TPF): 0.925 True Positive Fraction (FPF): 0.14	The model localizes bone loss areas with high classification effectiveness
4* Disease Detection	Lee et al., 2022 [57]	VGG+Individual CNN	Periapical Radiographs	1,740 images Train: 1,218 images Valid: 417 images Test: 105 images 1218 / 417 / 105	Bone loss	Acc: 0.99 AUC: 0.98	The proposed algorithm is helpful in diagnosing periodontal bone loss
	Krois et al., 2019 [36]	Seven Layered Deep CNN	Panoramic radiographs	1,750 images Train: 1,400 images Valid: 350 images 1400 / 350	Bone loss	Acc: 0.81	The model shows discrimination ability similar to that of dentists
	Kim et al., 2019 [35]	Deep CNN + Transfer Learning	Panoramic radiographs	12,179 images Train: 11,189 images Valid: 190 images Test: 800 images 1189 / 190 / 800	Bone loss	AUROC: 0.95 F1-score: 0.75 Sensitivity: 0.77 Specificity: 0.95 PPV: 0.73 NPV: 0.96	The model is useful in tooth numbering and achieved detection performance superior to that of dental clinicians
	Lee et al., 2019 [44]	GoogleNet InceptionV3 + Transfer Learning	Panoramic radiographs and CBCT images	2,126 images including 1,140 panoramic and 986 CBCT images Train: 1700 images Test: 426 images 1700 / 426	Odontogenic cyst lesion	Panoramic images: AUC – 0.847 Sensitivity – 0.882 Specificity – 0.77 CBCT images AUC – 0. 914 Sensitivity - 0.961 Specificity – 0.771	The model provides higher diagnostic performance on CBCT images in effectively detecting and diagnosing cystic lesions
Disease Classification	Moran et al., 2020 [47]	ResNet Inception	Periapical radiographs	467 images Train: 415 images Test: 52 images 415 / 52	Periodontal bone destruction	Acc: 0.81 Precision: 0.76 Recall: 0.92 Specificity: 0.71 NPV: 0.90	The inception model classifies regions based on the presence of periodontal bone destruction with encouraging performance

Table 2.2: Summary of related studies for AI application for disease segmentation, diagnosis and risk assessment

AI Application	Author, Year (Ref)	Architecture	Data Modality	Dataset Size Split (Train/ Val/Test or Train/ Test)	Study Factor	Results (Performance metrics/values)	Conclusion
Disease Segmentation	Khan et al., 2021 [52]	UNet + DenseNet121	Periapical radiographs	200 images Train: 160 images Test: 40 images	Bone recession and inter-radicular radioulency	mIoU: 0.501 Dice score: 0.569	Automates the process of detecting the presence and shape of caries
	Zheng et al., 2021 [50]	Automatically constrained dense U-Net	CBCT images	100 images	bone lesion identification	Dice score for different categories: Background: 0.961 Lesion: 0.709 Material: 0.822 Bone: 0.877 Teeth: 0.801	The model is helpful in detecting the correct shape of the lesion and the bone
	Duong et al., 2019 [34]	UNet	High frequency ultrasound images	35 images Train: 30 images Test: 5 images 30 / 5	Alveolar bone assessment	Dice Coefficient: 0.75 Sensitivity: 0.77 Specificity: 0.99	The method yields a higher performance in delineating alveolar bone as compared to experts
	Nguyen et al., 2020 [48]	U-Net with ResNet34 encoder	Intraoral ultrasound images	1,100 images Train: 700 images Valid: 200 images Test: 200 images 700 / 200 / 200	Alveolar bone assessment	Dice Coefficient: 0.853 Sensitivity: 0.885 Specificity: 0.998	The model has the potential to detect and segment alveolar bone automatically
3* Disease Diagnosis	Li et al., 2020 [46]	Mask RCNN + novel caliberation method	Panoramic radiographs	298 images Train: 270 images Test: 28 images 270 / 28	Periodontitis prediction	mAP: 0.826 Dice score: 0.868 F1-score: 0.454 Accuracy: 0.817	The model is useful for diagnosing the severity degrees of periodontitis
	Papantonopoulos et al., 2014 [10]	Multilayer Perceptron ANN	Textual	29 subjects	Aggressive periodontitis	Accuracy: 0.981	The model provides effective periodontitis classification
	Geetha et al., 2020 [42]	Back propagation Neural Network	Intraoral digital radiographs	105 images	Dental caries detection	Accuracy: 0.971 FPR: 2.8% ROC: 0.987	The model is helpful for the detection of tooth decay and is independent of visual errors
Risk Assessment	Shankarapillai et al. 2012 [8]	Multilayer Feedforward Propagation	Textual	230 subjects	Periodontitis risk assessment	MSE: 0.132	The model can be used for effective periodontitis risk prediction

Chapter 3

Design and Methodology

3.1 Introduction

This chapter includes detailed explanation of the deep learning based model proposed for dental caries diagnosis on intraoral periapical radiographs. Figures representing the dataset distribution and the proposed model are provided along with the details regarding the loss function employed for multi-class classification and localization of lesions. Additionally, details related to the performance measures adopted to analyze the performance of the proposed deep learning mechanism are provided in the following sections.

3.2 Proposed Methodology

3.2.1 Overview

The process flow of the proposed dental lesion detection is shown in Fig. 3.1. First, the collected annotated images are preprocessed to remove noise, enhance contrast and improve resolution of the images. Next, the preprocessed images are used by the proposed lightweight backbone network for feature extraction, the extracted feature maps are then forwarded to the region proposal network (RPN) that generates region proposals using the feature maps and forwards it to the ROI align block, this block processes both the feature maps and region proposals and classifies the input image using fully connected layers. The model further exhibits the bounding box on the identified region so it can be visualized.

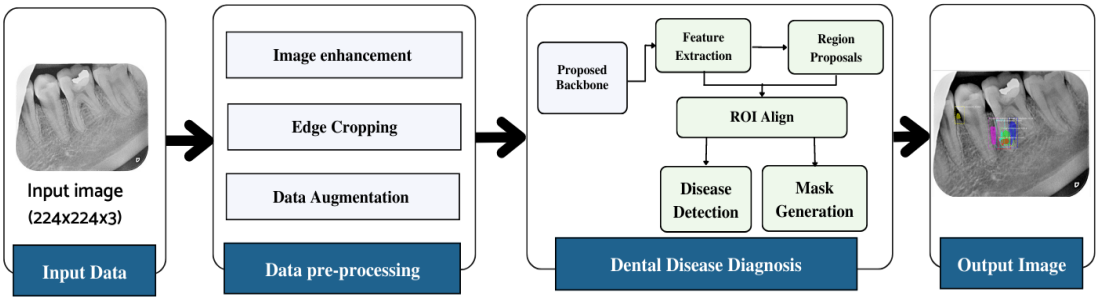

Figure 3.1: Proposed process flow

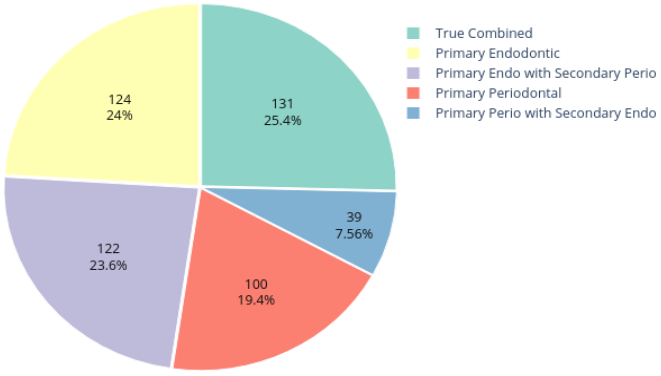

Figure 3.2: Dataset distribution

3.2.2 Dataset Analysis and Preprocessing

The dataset employed for this study was obtained from the Armed Forces Institute of Dentistry, Rawalpindi Pakistan. A total of 534 periapical images were collected out of which 516 were labeled by experienced radiologists and dentists. The dataset distribution is shown below in Fig. 3.2.

The ground truth of the obtained images was generated using VGG Image Annotator (VIA) tool [65]. Five types of lesions were localized manually using bounding polygons around the carious regions. The annotations were saved in a JSON file, where each mask represents a set of polygon points. The pixels inside the bounding polygons corresponding to lesions were assigned values of 1 for primary endodontic, 2 for primary endo with secondary perio, 3 for primary periodontal, 4 for primary perio with secondary endo, and 5 for true combined, while the rest of the pixels were regarded as background with a value of 0. For each labeled data, there is corresponding instance information as illustrated in Fig. 3.3.

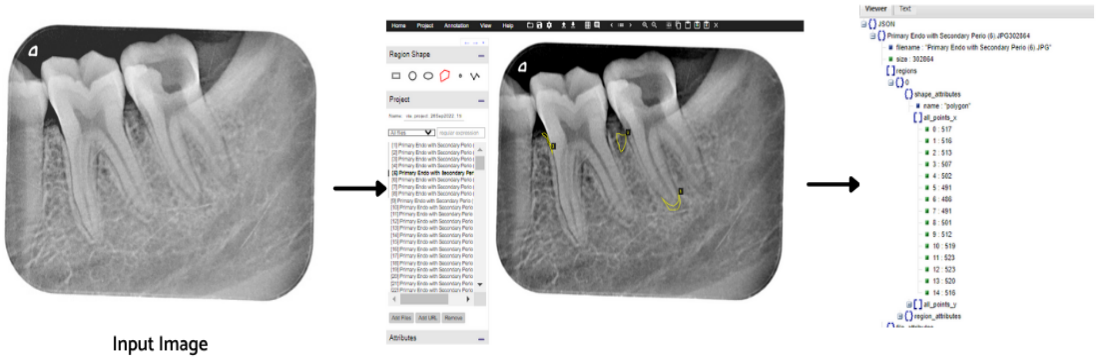

Figure 3.3: Image labeling process using VIA tool

The annotated image dataset is preprocessed to improve image quality and remove noise in radiographic images. The influence of image preprocessing has been analysed in several studies. Tian et al. found that image enhancement leads to better performance of fast R-CNN for detection tasks [31]. Chen et al. evaluated image enhancement on RGB images followed by deep learning based method for accurate prediction of retinal blood vessels [40]. In a more recent attempt, Pannetta et al. [59] tested different image enhancement techniques such as Histogram equalization (HE) [1], Contrast Limited Adaptive Histogram Equalization (CLAHE) [68], Dynamic Fuzzy Histogram Equalization (DFHE) [7], Guided filtering (GF) [15], and Bi-Histogram Euqalization (BBHE) [9] on medical image dataset. It was found that CLAHE performs better in comparison to other techniques to enhance image contrast of the images. This study utilizes CLAHE to enhance image contrast to improve the performance of the proposed lightweight disease detection and localization model.

3.2.3 Lightweight Mask RCNN

The training process of M-RCNN requires high-performance computing resources to learn and analyze substantial information obtained from medical imagery. To reduce the performance requirement of M-RCNN and ensure that it operates properly, a lightweight backbone network is utilzied with M-RCNN to classify five types of endo-perio lesions. The focus of this research is to propose a lightweight M-RCNN model that can operate on platforms with less computational resources such as graphic process unit (GPU) and memory and provide performance similar to that of the original M-RCNN [60].

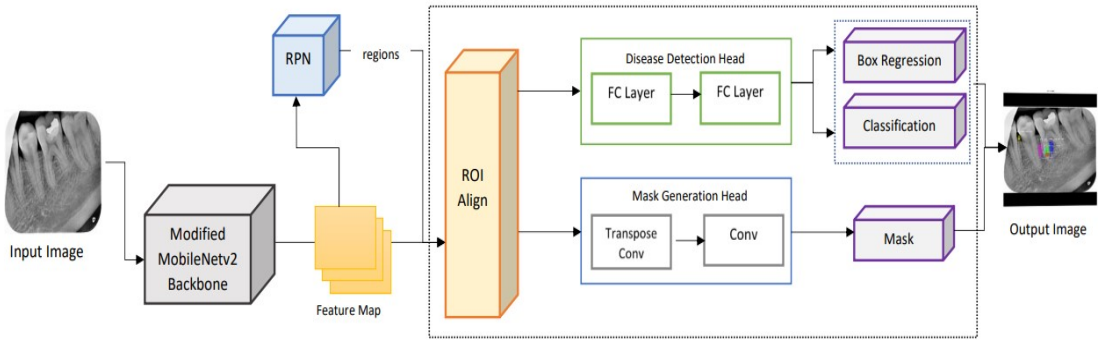

Figure 3.4: Architecture of Lightweight M-RCNN with Modified MobileNet-v2 as backbone

For this purpose, a lightweight network MobileNet-v3 is utilized for feature extraction followed by a depthwise separable convolutional layer proceeding tiny region proposal network (RPN) to extract candidate regions with potential targets [55]. The RPN generates anchor boxes for each classified object using the softmax activation function. The extracted proposal regions along with feature maps are applied to ROI alignment to locate all the feature map areas. ROI alignment wraps different feature vectors which are then applied to mask generation and classification. The fully connected layer provides classification and bounding boxes for each identified endo-perio lesion. The masks are generated by the convolution layer for each object at the pixel level. The proposed framework for lightweight M-RCNN for dental lesion classification and localization is depicted in Fig. 3.4.

3.2.4 Backbone Network

To reduce the number of parameters in the proposed lightweight M-RCNN, MobileNet-v2 is employed, which extends MobileNet-v1 and is faster with 30% fewer parameters [67]. In MobileNet-v2 [28], an inverted residual structure is introduced to reduce complexity and increase the speed. The employed backbone network comprises two layers with the first layer of 1x1 pointwise convolution with ReLU6 and a depthwise convolutional layer. The inverted design of the employed MobileNet-v2 makes the model considerably memory efficient and improves overall performance. The structure of the employed MobileNet-v2 is illustrated below in Fig. 3.5. The layers of the proposed backbone network are shown in Fig. 3.6

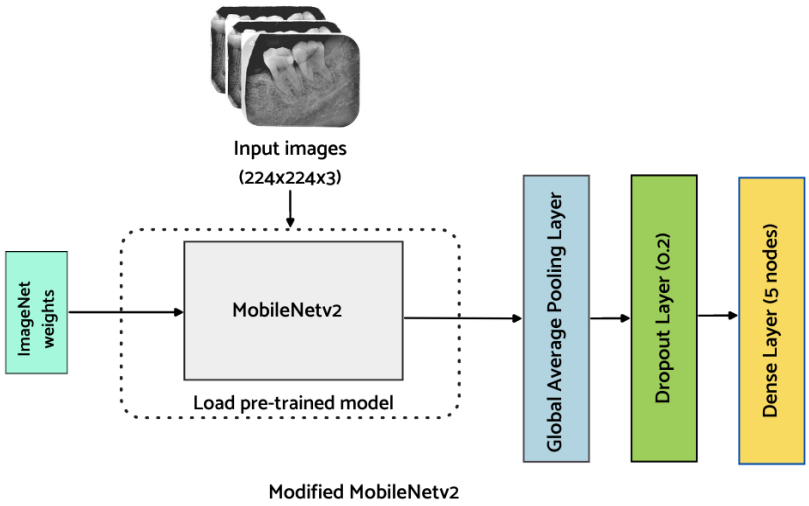

Figure 3.5: Proposed Backbone Network (Modified MobileNet-v2)

mobilenetv2_1.00_224_input InputLayer	input: output:	[(None, 224, 224, 3)]	[(None, 224, 224, 3)]
mobilenetv2_1.00_224 Functional	input: output:	(None, 224, 224, 3)	(None, 7, 7, 1280)
global_average_pooling2d_4 GlobalAveragePooling2D	input: output:	(None, 7, 7, 1280)	(None, 1280)
dropout_2 Dropout	input: output:	(None, 1280)	(None, 1280)
dense_6 Dense	input: output:	(None, 1280)	(None, 128)
dense_7 Dense	input: output:	(None, 128)	(None, 5)

Figure 3.6: Layers of the Proposed Backbone Network

For the classification of endo-perio lesions, MobileNet-v2 modified with additional layers proposed by Kolonne et al. [53] is utilized in this work. To avoid impairment of already learned features, the base layers are frozen. Additionally, the fully connected layer of MobileNet-v2 is replaced with a Global average pooling layer which calculates the average value of each feature map in the convolutional layers and sums the spatial information of the input images. Additionally, a dropout layer is added to minimize the model from overfitting. Finally, a dense layer is added for the classification of endo-perio lesions. The model weights are saved after fine-tuning the hyperparameters of the model to improve the classification results. As this is a multi-class classification problem, Softmax is used as an activation function in the output layer to predict the probability for each of the five classes and is defined below:

$$\sigma(z) = \frac{1}{1 + e^{-z}} \tag{3.2.1}$$

3.2.5 Region Proposal Network (RPN)

Once the multi-scale features are extracted using the proposed lightweight backbone network, the feature maps are passed onto Regional Proposal Network (RPN). The RPN detects regions and matches those regions to the ground truth. The region proposals are predicted simultaneously at each sliding window, where k represents the maximum possible proposals at each location. Additionally, k proposals are parameterized for each proposal to form anchors [13]. Due to the small size of the regions to be localized in the periapical radiographs, the anchor sizes and anchor aspect ratios were selected after extensive experimentation to fit the task at hand adequately [51]. The anchors are matched to the ground truth based on the intersection over union (IoU) between the anchor and the ground truth. The anchors are linked to the ground truth boxes and are assigned to the foreground once IoU exceeds the defined threshold which is 0.7 in this study. If the IoU is below the defined threshold, the identified region is ignored. The proposal regions with IoU higher than a threshold are considered as foreground. This block provides several regions of interest (ROI) which are then utilized by ROI alignment to identify where these regions of interest lie in the feature maps. The structure diagram of RPN is illustrated below in Fig. 3.7.

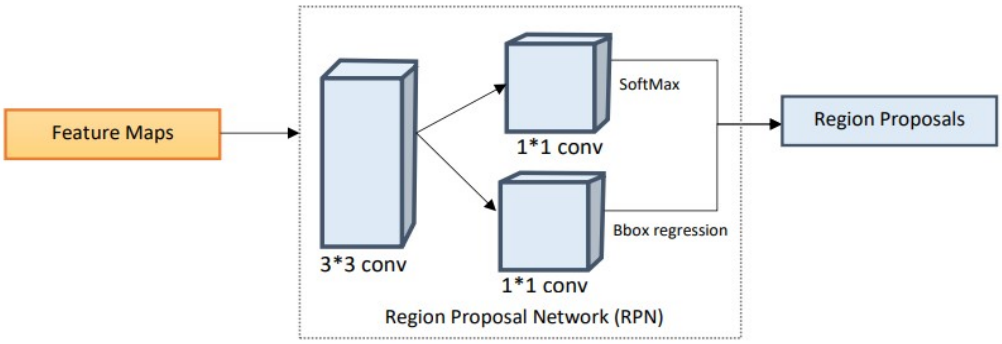

Figure 3.7: Structural Diagram of Region Proposal Network (RPN)

3.2.6 Region of Interest (ROI) Alignment

ROI Align extracts feature vectors from the feature map based on the region of interests identified by RPN [69]. These feature vectors are turned into fixed-sized tensors to be processed further. The ROI is scaled with their corresponding areas based on the regions' location, scales, and aspect ratios. To ensure uniformity, the samples are aligned over feature map areas. After generating the region proposals, the next block involves making predictions by taking ground truth boxes, feature maps generated by the proposed lightweight backbone network, and region proposals generated by RPN. Additionally, the results represented by ROI feature maps are then processed by two parallel branches: disease detection and mask generation.

- Disease Detection Head: Using the ROI feature map, the disease category is predicted along with refined instance boundary box. This branch contains two fully connected (FC) layers to map the feature vector to the classes and instance bounding box coordinates.
- Mask Generation Head: The ROI feature map is fed into a transposed convolutional layer followed by another convolutional layer. The segmentation masks are generated for the classes and the output mask is selected according to the class prediction provided by the disease detection branch.

3.3 Loss Function

A multiclass loss function for the proposed lightweight Mask-RCNN is used which combines the loss of classification, localization and segmentation mask and calculated as shown in Eq. 3.3.1:

$$L = L_{cls} + L_{box} + L_{mask} \tag{3.3.1}$$

where L_{cls} and L_{box} are similar to Faster-RCNN and are used as loss functions in both BBox regression and classification. Additionally, L_{mask} generates mask of dimension $K \times m \times m$ for each RoI extracted after RPN and classifies each pixel for corresponding classes and K represents the number of classes to be classified which is five in this case.

3.4 Performance Measure

The performance of the proposed model is measured based on different performance indicators. For evaluation of the model's classification, classification accuracy, area under receiving operating characteristic curve (AUC) are chosen and are represented in Eq. 3.4.1 and 3.4.2, 3.4.3.

$$Accuracy = \frac{TP + TN}{TP + FN + TN + FP} \tag{3.4.1}$$

$$Sensitivity = Recall = \frac{TP}{TP + FN} \tag{3.4.2}$$

$$Specificity = \frac{TN}{FP + TN} \tag{3.4.3}$$

where AUC is calculated as area under the $Sensitivity - (1 - Specificity)$ curve . To detect and evaluate detection performance of the proposed model, mean average precision (mAP), mean average recall (mAR), F1-score are chosen. The mAP, mAR and F1-score are calculated as represented in Eq. 3.4.4, 3.4.5, and 3.4.6 respectively.

$$mAP = \frac{1}{N} \sum_{i=1}^{N} AP_i \tag{3.4.4}$$

$$mAR = \int_{0.5}^{1} recall(o)do \tag{3.4.5}$$

$$F1 - score = \frac{2 \times (mAP \times mAR)}{mAP + mAR} \tag{3.4.6}$$

where average precision (AP) is calculated for each class and then the average is taken over N classes to calculate mAP [66]. A trade-off between precision and recall is considered along with both false positives and false negatives (FN). The calculation of mAR is similar to mAP, however, the recall for mAR is calculated for different IoU thresholds [21] and is calculated as two times the area under the recall IoU curve averaged over IoU ranging between 0.5-1. After calculating mAP and mAR, F1-score is calculated using mAP and mAR respectively.

3.5 Summary

This chapter demonstrates the proposed deep learning based model for detection and identification of periapical lesions. Details regarding dataset collection, and preprocessing are discussed. As this research is targeting multi-class, the loss function adopted is discussed in the above sections. To measure the performance of the proposed model, performance indicators are considered. The adopted performance metrics to be used for analysis of the proposed model are also briefly explained. Using the model discussed in this chapter can aid in identification of dental disease and help dental clinicians in diagnosing periapical lesions.

Chapter 4

Implementation and Results

4.1 Introduction

For comparison, the proposed Mask RCNN based on lightweight MobileNet-v2, and the base RCNN is trained under the same environment. In the collected dataset, each image belongs to one of the disease classes. The custom-made dataset is used to train the proposed model. The images within the dataset are divided as 80% for training, 10% for validation, and the remaining 10% for testing. The images within the dataset belong to one of the disease types (Primary endo with secondary perio, primary periodontal, primary perio with secondary endo, primary endodontic, and true combined) lesions have been utilized. To reduce the computational time and increase the efficiency of Mask-RCNN, a modified lightweight pretrained Mobilenet-v2 is employed as the backbone network of Mask-RCNN. Different values for hyperparameters are employed to see the performance of the proposed model on the disease detection dataset. To ensure an effective comparative experiment, the hyperparameters for testing different backbone networks with Mask-RCNN are kept consistent. The following subsections explain the experimental settings, the ablation experiment conducted to see how the proposed model performs with different backbone networks, and the performance evaluation of the proposed model on the test dataset.

Table 4.1: Parameter Configuration for this experiment

Weight Decay	**Learning Rate**	**Min Detect Confidence**	**Epoch**	**Batch Size**
0.0001	0.001	0.7	50	2
Validation Steps	**Steps per Epoch**	**Learning Momentum**	**RPN Anchor Scale**	**BBOX Standard Deviation**
50	200	0.9	(8, 16, 64, 128, 256)	[0.1 0.1 0.2 0.2]

4.2 Experiment Setting

For conducting experiments, a laptop equipped with an intel i7-1165G7 processor (2.80 GHz), 8GB RAM is utilized. Additionally, the code was implemented on Google Colab equipped with Python 3.5, Tensorflow 1.14.0, and Keras 2.2.5.

Additionally, the configurations employed in the implementation of the model are shown below in Table. 4.1.

4.3 Dataset Preprocessing

To enhance the small details, local contrast, and texture of medical images, CLAHE [16] is used. Different tile regions of the image based on the histogram are computed using CLAHE. The local details of the radiograph are enhanced by limiting histogram amplification and clipping of the histogram. Additionally, CLAHE allows reducing over-amplification of noise within x-ray images and serves as a better alternative fro image enhancement compared to manula dileanation methods [49]. The process of CLAHE is carried out in two steps: First, the image is divided into non-overlapping regions that are equal in size followed by obtaining the clip limit for the clipping histogram. In the second step, the histogram is redistributed so that the height remains under the clip limit. The results obtained using CLAHE are illustrated in Fig. 4.1.

After the image has been preprocessed, the mask generated for the images from json file in the collected dataset is overlaid on the original images. A visualization of the mask predicted using the proposed M-RCNN on the collected disease dataset is illustrated in Fig. 4.2.

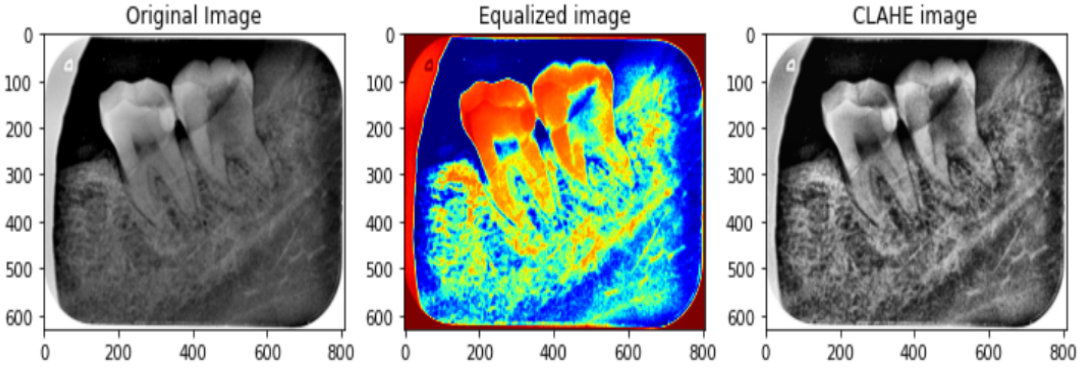

Figure 4.1: Preprocessed image sample with CLAHE

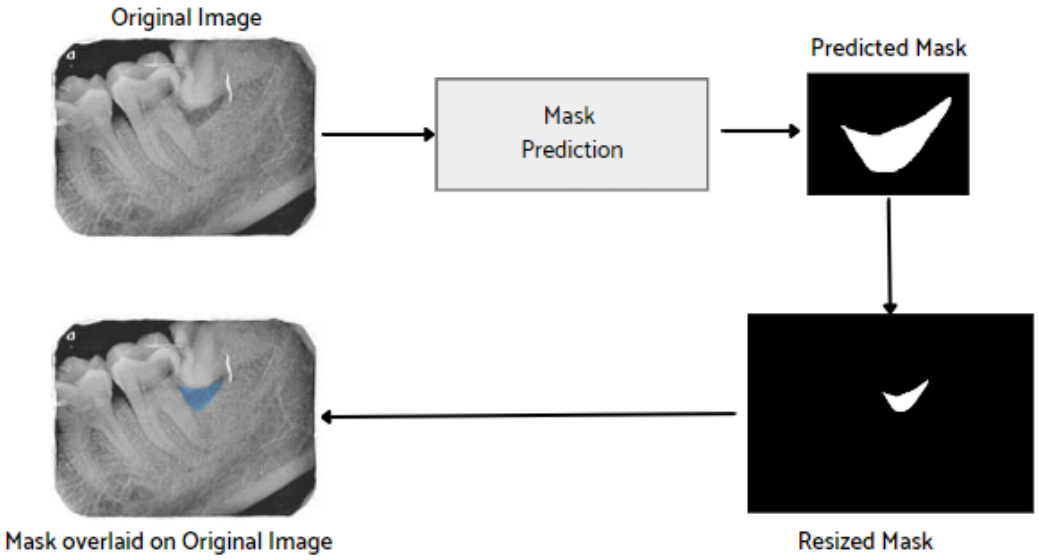

Figure 4.2: Mask overlaid on original image

Table 4.2: Comparison of M-RCNN with different backbone networks

Model	Backbone Network	Precision	Recall	F1-score	ROC AUC
Mask-RCNN	ResNet-50 [45]	0.82	0.83	0.78	0.614
	ResNet-101 [25]	0.81	0.84	0.74	0.670
	MobileNet-v2 [62]	0.86	0.87	0.84	0.721
	Proposed Backbone Network	**0.86**	**0.89**	**0.89**	**0.805**

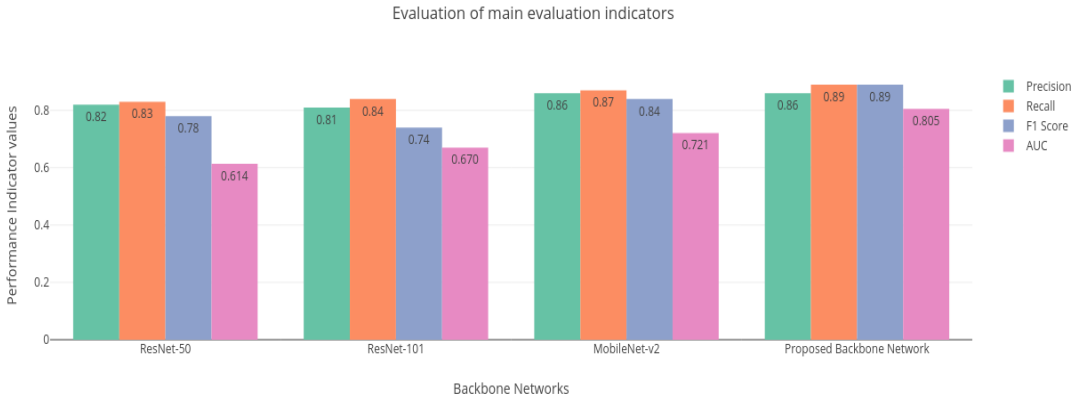

Figure 4.3: Evaluation of main evaluation indicators for different backbone networks

4.4 Ablation Experiment

To further examine the effectiveness and contribution of the proposed method, additional ablation experiments are conducted [30]. The aim of the ablation experiment is to provide deeper insights into the improvements obtained by the proposed model. The proposed model is built and trained using Tensorflow, which is an open resource deep learning application programming interface (API). For comparison of the backbone networks, the hyperparameters are kept consistent (optimizer 'Adam' is chosen with a learning rate of 0.0001 and loss function 'categorical cross entropy). Additionally, to prevent the model from overfitting, early stooping is applied. The results obtained from the ablation studies are shown in Table. 4.2. Additionally, the comparison of the experimental results using different backbones is shown in Fig. 4.3.

The performance of Base Mask-RCNN is evaluated in regards to the evaluation metrics like precision, recall, mean average precision (mAP), and area under the curve (AUC).

Table 4.3: Comparison of performance indicators for each disease

Class	Accuracy	Precision	Recall	F1-score
Primary Endo with Secondary Perio	0.89	0.83	0.75	0.77
Primary Periodontal	0.96	0.80	1.00	0.75
Primary Perio with Secondary Endo	0.87	0.91	0.90	0.91
Primary Endodontic	0.92	0.94	0.86	0.89
True Combined	0.97	0.87	0.89	0.88
Average	**0.93**	**0.86**	**0.89**	**0.89**

It is evident from Table. 4.2, that the proposed modified lightweight Mobilenet-v2 performs accurately compared to other models like ResNet-50 and ResNet-101 that are employed by the base Mask-RCNN, achieving an overall precision of 0.86, recall of 0.89, mAP of 0.85, and ROC AUC of 0.805 for detection and classification of five types of disease while reducing the number of parameters compared to the base Mask-RCNN.

Additionally, the performance of the proposed model was evaluated based on well-known performance indicators, the result of the proposed model for each classified disease are shown below in Table. 4.3. The performance parameters indicate that the proposed backbone network provides good performance for disease classification.

4.5 Performance Evaluation

4.5.1 Comparison with Different Backbone Networks

To demonstrate the performance superiority of the proposed model, the previous section discusses the experiments conducted to show the performance comparison of different backbone networks with M-RCNN based on consistent hyperparameters. The results indicate that the proposed backbone network performs better than other state-of-the-art networks employed as the backbone with M-RCNN. However, to further validate the proposed model's precision and accuracy, it is compared with the Base M-RCNN with ResNet-50 and resnet-101 backbone networks. The proposed and comparison model is tested on different periapical radiographic images.

For the evaluation of the proposed lightweight M-RCNN, the collected dataset is divided

into train, valid, and test sets. In the dataset, For comparison, the proposed model is compared with Base M-RCNN with ResNet-50 backbone network and M-RCNN with ResNet-101 backbone network. The parameter configuration for the experiment is shown in Table. 4.1. in the process of training, the learning rate was set to 0.01 which was then adjusted to 0.001, the weight decay was set to 0.0001, learning momentum of 0.9. In medical images, the localized regions are often smaller in size, to fit the disease regions more accurately in this study, the RPN anchor scale was set to (8,16, 64, 128, 256), and the BBOX standard deviation of [0.1 0.1 0.2 0.2]. The model is trained for 50 epochs and due to the small dataset, the batch size was kept at 2 with 50 validation steps, and 200 steps per epoch.

4.5.2 Comparison with Test Images

To verify the effectiveness of the model, two performance indicators, mean average precision (mAP) and mean intersection over union (IoU) is used. Fig. 4.4. below shows the comparison of the precision-recall curve of the Mask RCNN with two different backbone networks which include ResNet-50 and ResNet-101. The results form Table. 4.4 indicate that the proposed Mask-RCNN with lightweight modified MobileNet-v2 backbone network and RPN based region detectiona achieved mAP (0.85) which is higher compared to other compared models, Mask RCNN with ResNet-50 [45] with mAP (0.71), ResNet-101 [24, 20] (0.74), ResNet-101 with FCN based region detection [38] (0.67), and Faster RCNN with ResNet-50 [63] (0.80). The performance comparison of the proposed model with other models proposed for disease detection and localization is provided in Table. 4.4.

4.6 Accuracy and Loss Comparison

This study draws motivation from the current research initiatives on detection and localization of dental disease with a view of using deep learning networks. The proposed Mask RCNN with a proposed lightweight modified MobileNet-v2 backbone model were trained on 10 to 50 epochs respectively. The model outputs the location of the lesion diagnosed and the intensity of the lesion by segmenting the area that contains lesion. Additionally, the proposed model calculates the area ratio of the bounding boxes and area of interest surrounding the detected lesion. The graphs of the training and valida-

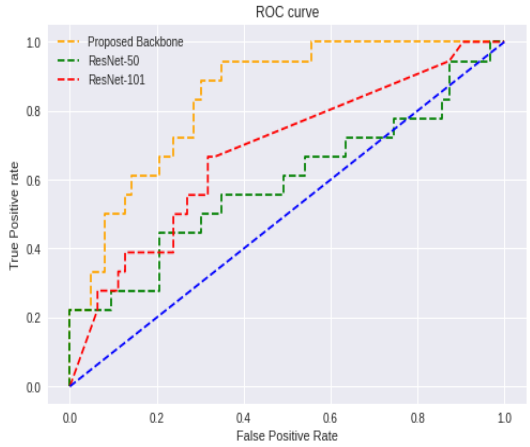

Figure 4.4: ROC-AUC curve of different backbone networks for M-RCNN

Table 4.4: Comparison of measurement index of different networks for disease localization

Model	Variation	mean Average Precision (mAP)	mean Insection over Union (mIoU)
Mask-RCNN	ResNet-50 [45]	0.71	0.70
	ResNet-101 [24, 20]	0.74	0.68
	ResNet101 backbone and FCN based region detection [38]	0.67	0.58
Faster RCNN	ReNet-50 [63]	0.80	0.69
Mask-RCNN	**Lightweight Modified MobileNet-v2 backbone with RPN based region detection**	**0.85**	**0.71**

Figure 4.5: Accuracy and loss of proposed model

tion accuracy and loss for proposed model are shown in Fig. 4.5 a and b. It can be seen that the model shows an increasing trend for accuracy and decreasing trend in terms of training loss as the number of epochs increases. To avoid the mode from overfitting, early stopping was applied.

The proposed model accurately predicts and localizes the lesions as depicted in Figures 4.6 to 4.10. The results indicate that the model makes predictions similar to that of the annotated masks using the periapical radiographic images. Additionally, the proposed model was evaluated based on performance indicators like precision, recall, F1-score, and accuracy for each classified periodontal lesion. The results for each lesion are shown in Table. 4.3. The obtained results indicate that the proposed backbone network provides good performance for disease classification.

Compared to different backbone networks as shown in Table. 4.2, the proposed model performs better compared to other detection and localization methods precision (86%) recall (89%), F1-score (89%), and AUC (0.805). The results show the efficiency of the proposed model and exhibit the efficiency of the proposed model for lesion detection outweighing other state-of-the-art approaches for disease identification and localization.

To verify the effectiveness of the model, two performance indicators, mean average precision (mAP) and mean intersection over union (IoU) is used. Fig. 4.4. below shows the comparison of the precision-recall curve of the Mask RCNN with two different backbone networks which include ResNet-50 and ResNet-101. The results from Table. 4.4 indicate that the proposed Mask-RCNN with lightweight modified MobileNet-v2

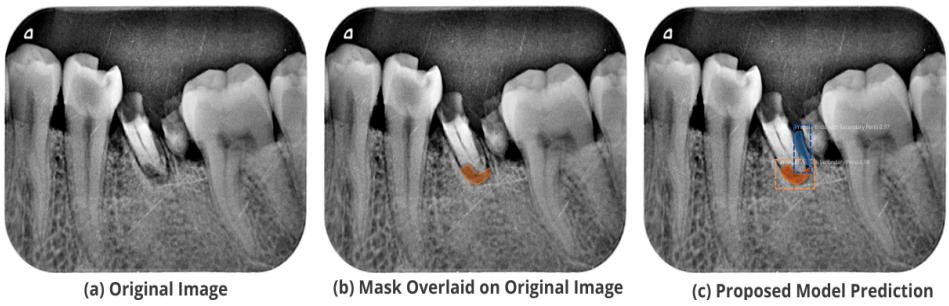

Figure 4.6: Test Performance for localization of Primary Endo and Secondary Perio lesion

Figure 4.7: Test Performance for localization of Primary Endodontic lesion

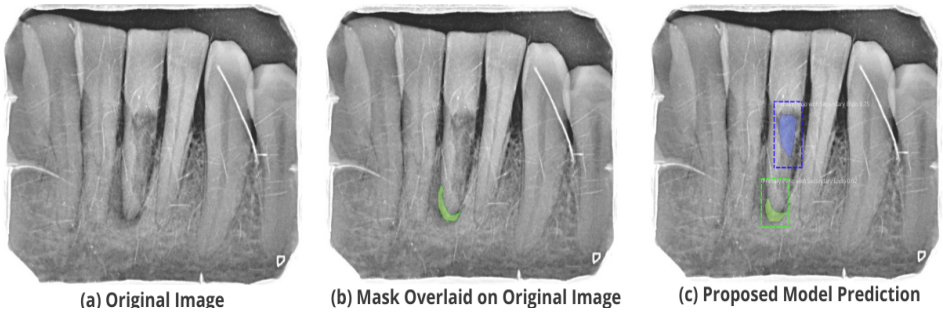

Figure 4.8: Test Performance for localization of Primary Perio and Secondary Endo lesion

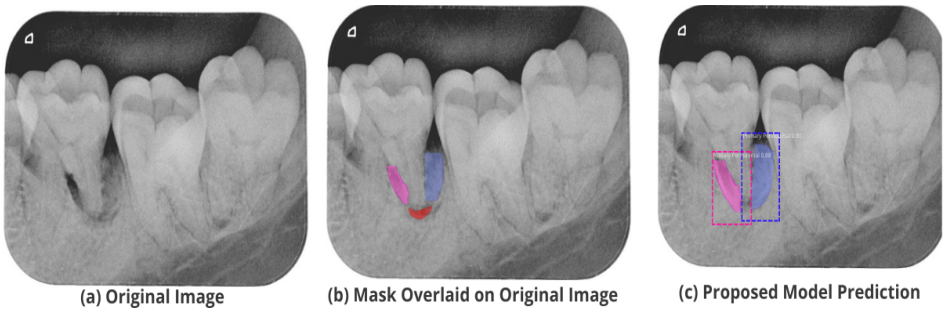

Figure 4.9: Test Performance for localization of Primary Periodontal lesion

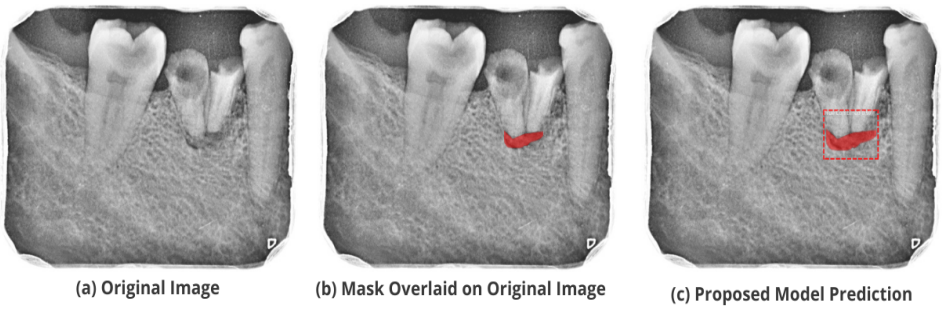

Figure 4.10: Test Performance for localization of True Combined lesion

backbone network and RPN based region detection achieved mAP (0.85) which is higher compared to other compared models, Mask RCNN with ResNet-50 [45] with mAP (0.71), ResNet-101 [24, 20] (0.74), ResNet-101 with FCN based region detection [38] (0.67), and Faster RCNN with ResNet-50 [63] (0.80).

The figures 4.6 to 4.10 depict the location at which the disease has been classified along with the confidence of the disease type detected. Fig. 4.6 a to c shows the original image, the mask overlaid on the original image, and the model prediction. It can be seen that the model predicts the lesion accurately and displays the lesion name, confidence, and detection box to localize the lesion. Similarly, Fig. 4.7c localizes primary endodontic lesion, it can be seen that the proposed model detects and localizes this lesion accurately and identifies another region as highlighted in red in 4.7c. The results obtained by the proposed model for primary perio with secondary endo lesion are depicted in Fig. 4.8c, it can be seen that the model detected an additional region highlighted in blue. Fig. 4.9c indicates the results obtained from the proposed model for primary periodontal lesion, it can be seen that the region with the lesion in question are highlighted with confidence. Finally, the model localizes true combined lesion as illustrated in Fig. 4.10c and highlights the region where the lesion is detected.

4.7 Summary

Overall, it is evident from the images, that the proposed model provides higher classification accuracy compared to other approaches used within the dental disease localization domain. It can be visualized that the proposed Mask RCNN with lightweight MobileNet-v2 provides better detection of dental disease in radiographic images and positions the

frames more accurately. To further validate the robustness of the proposed model for dental lesion detection, different test images are selected to show the visual performance of the proposed model compared with the ground truth and other state-of-art methods like Mask-RCNN with ResNet-50 [45], ResNet-101 [24], ResNet-101 with FCN based region detection [38] and Faster RCNN [63]. The proposed model provides good detection and localization performance for five types of periodontal lesions. This chapter highlights the performance of the proposed model in terms of loss and accuracy along with discussion related to the test images to evaluate the performance of the proposed model. It is evident from the analysis that the proposed model outperforms state-of-the-art methods for identification of small regions with dental lesions. However there are certain limitations that need consideration to further enhance the performance of the proposed model. This chapter highlights these limitations to pave way for future research in this regard.

Chapter 5

Conclusion

Due to the outbreak of COVID-19, several countries have been affected, leading to a global emergency. The rise in COVID-19 has brought challenges in maintaining patients' dental health and providing urgent dental care to mitigate risks of missed diagnosis. Artificial intelligence (AI) has evolved rapidly in terms of complexity, diversity, and computational capabilities, especially in medicine [62, 64]. AI has emerged as one of the prospective technologies in healthcare, making significant progress in predictive machine learning models for dental care [54]. The potential applications of AI apply to dental practices and play a significant role in practice management. Dental clinicians may deploy AI systems as a supplemental tool in providing precise dental diagnoses and planning treatments.

Moreover, different techniques implemented to aid in dental disease diagnosis have led to the introduction of different imaging systems, including x-ray radiography intraoral and extraoral imaging. X-ray imaging systems have become a norm in dentistry for identifying dental lesions, normal and abnormal dental structures, and predicting treatment outcomes. However, a safer method with non-ionizing radiation is also employed by dentists for diagnosing caries and lesions, known as near-infrared imaging. In dentistry, dental ailments are primarily identified using images of the oral cavity each shot from a different angle; a process that is largely manual. Thus, human inference plays a significant role in analyzing x-ray imagery to recognize dental structures, bone loss, and cavities. However, human intervention is prone to error. Thus, there is a need of system that can help dentists in analyzing radiographs and identify lesions more efficiently.

This study proposes a detection and localization network based on deep learning for

classification and localization of different periodontal lesions on periapical radiographic images. For feature map extraction, a lightweight modified MobileNet-v2 by adding a global average pooling layer, dropout layer is utilized to enhance the performance of the Mask-RCNN model followed by region proposal network (RPN) for identification of region proposals. The proposed mechanism provides multi-disease prediction by obtaining anchor boxes. Additionally, hyperparameters are fine tuned to further improve the performance of the model and acquire accurate predictions. The presented system detects periapical lesions that are tough to recognize by other existing method due to complex nature of radiographic images. The images are preprocessed using CLAHE to enhance image contrast and reduce noise to gain better performance. The proposed model is tested on a custom-made dataset with annotated disease labels. The masks are generated using the provided annotations which are then utilized to train the model. The results indicate that the proposed model is found helpful in identification and localization of periapical disease with an average mean average precision (mAP) of 80% superior to other existing dental disease localization solutions on radiographic images.

5.1 Limitations

The proposed model provides good performance for periapical lesion detection on intraoral periapical radiographs, however there are certain limitations to the proposed approach that need addressing to further improve the model, these are:

- The dataset used to train the proposed model is small in terms of size. In this work, image augmentation is used for better classification accuracy. The model performance may improve further by employing a larger annotated dataset with multiple lesions.
- The proposed model is tested on only intraoral radiographic images, further research is required to train the model on colored images and analyze its performance.

5.2 Future Work

Further studies are needed to improve the performance of the proposed model.

- A bigger dataset can be employed for feature regularization on periapical radiographic images.
- This work can be extended further by embedding Internet of Things (IoT) for data collection and make the proposed mechanism widely accessible.
- The proposed model's performance can be analyzed on other radiographic datasets like panoramic radiographs, colored images, and a hybrid dataset combining both radiographic and colored images.
- In this work, for preprocessing radiographic images, CLAHE is used. Other image enhancement methods can be employed and compared to analyze the performance of the proposed model.

Bibliography

[1] Stephen M. Pizer et al. “Adaptive histogram equalization and its variations”. In: *Computer Vision, Graphics, and Image Processing* 39.3 (Sept. 1987), pp. 355–368. DOI: 10.1016/s0734-189x(87)80186-x.

[2] William G Baxt. “Application of artificial neural networks to clinical medicine”. In: *The lancet* 346.8983 (1995), pp. 1135–1138.

[3] Anil K Jain, Jianchang Mao, and K Moidin Mohiuddin. “Artificial neural networks: A tutorial”. In: *Computer* 29.3 (1996), pp. 31–44.

[4] Imad A Basheer and Maha Hajmeer. “Artificial neural networks: fundamentals, computing, design, and application”. In: *Journal of microbiological methods* 43.1 (2000), pp. 3–31.

[5] Stefan Oprea et al. “Image processing techniques used for dental x-ray image analysis”. In: *2008 31st international spring seminar on electronics technology*. IEEE. 2008, pp. 125–129.

[6] Simon Haykin. *Neural networks and learning machines, 3/E*. Pearson Education India, 2009.

[7] Debdoot Sheet et al. “Brightness preserving dynamic fuzzy histogram equalization”. In: *IEEE Transactions on Consumer Electronics* 56.4 (Nov. 2010), pp. 2475–2480. DOI: 10.1109/tce.2010.5681130.

[8] Rajesh Shankarapillai et al. “Periodontitis risk assessment using two artificial neural network algorithms–a comparative study”. In: *International Journal of Dental Clinics* 4.1 (2012), pp. 17–21.

[9] Sayali Nimkar, Sucheta Shrivastava, and Sanal Varghese. “Contrast Enhancement and Brightness Preservation Using Multi-Decomposition Histogram Equalization”.

In: *Signal Image Processing : An International Journal* 4.3 (June 2013), pp. 83–93. DOI: 10.5121/sipij.2013.4308.

[10] Georgios Papantonopoulos et al. "Artificial neural networks for the diagnosis of aggressive periodontitis trained by immunologic parameters". In: *PloS one* 9.3 (2014), e89757.

[11] Soma Datta and Nabendu Chaki. "Detection of dental caries lesion at early stage based on image analysis technique". In: *2015 IEEE International Conference on Computer Graphics, Vision and Information Security (CGVIS)*. IEEE, Nov. 2015. DOI: 10.1109/cgvis.2015.7449899.

[12] PL Lin et al. "Alveolar bone-loss area localization in periodontitis radiographs based on threshold segmentation with a hybrid feature fused of intensity and the H-value of fractional Brownian motion model". In: *Computer methods and programs in biomedicine* 121.3 (2015), pp. 117–126.

[13] Shaoqing Ren et al. "Faster R-CNN: Towards Real-Time Object Detection with Region Proposal Networks". In: *CoRR* abs/1506.01497 (2015). arXiv: 1506.01497. URL: http://arxiv.org/abs/1506.01497.

[14] Ainas A ALbahbah, Hazem M El-Bakry, and Sameh Abd-Elgahany. "A new optimized approach for detection of caries in panoramic images". In: *International Journal of Computer Engineering and Information Technology* 8.9 (2016), p. 166.

[15] H. Geethu, S. Shamna, and Jubilant J. Kizhakkethottam. "Weighted Guided Image Filtering and Haze Removal in Single Image". In: *Procedia Technology* 24 (2016), pp. 1475–1482. DOI: 10.1016/j.protcy.2016.05.248.

[16] Kitti Koonsanit et al. "Image enhancement on digital x-ray images using N-CLAHE". In: *2017 10th Biomedical Engineering International Conference (BMEiCON)*. IEEE, Aug. 2017. DOI: 10.1109/bmeicon.2017.8229130.

[17] Jufriadif Na'am et al. "Image processing of panoramic dental X-ray for identifying proximal caries". In: *TELKOMNIKA (Telecommunication Computing Electronics and Control)* 15.2 (2017), pp. 702–708.

[18] Shreyansh A. Prajapati, R. Nagaraj, and Suman Mitra. "Classification of dental diseases using CNN and transfer learning". In: *2017 5th International Symposium on Computational and Business Intelligence (ISCBI)*. IEEE, Aug. 2017. DOI: 10.1109/iscbi.2017.8053547.

[19] Vitri Tundjungsari et al. “Investigating clinical decision support systems success factors with usability testing”. In: *International Journal of Advanced Computer Science and Applications* 8.11 (2017).

[20] Rajaram Anantharaman, Matthew Velazquez, and Yugyung Lee. “Utilizing Mask R-CNN for Detection and Segmentation of Oral Diseases”. In: *2018 IEEE International Conference on Bioinformatics and Biomedicine (BIBM)*. IEEE, Dec. 2018. DOI: 10.1109/bibm.2018.8621112.

[21] Badruswamy. “Evaluating Mask R-CNN Performance for Indoor Scene Understanding”. In: 2018.

[22] Andrew Collins and Yin Yao. “Machine learning approaches: data integration for disease prediction and prognosis”. In: *Applied Computational Genomics*. Springer, 2018, pp. 137–141.

[23] Geoffrey Hinton. “Deep learning—a technology with the potential to transform health care”. In: *Jama* 320.11 (2018), pp. 1101–1102.

[24] Gil Jader et al. “Deep Instance Segmentation of Teeth in Panoramic X-Ray Images”. In: *2018 31st SIBGRAPI Conference on Graphics, Patterns and Images (SIBGRAPI)*. IEEE, Oct. 2018. DOI: 10.1109/sibgrapi.2018.00058.

[25] Jeremiah W. Johnson. “Adapting Mask-RCNN for Automatic Nucleus Segmentation”. In: *CoRR* abs/1805.00500 (2018). arXiv: 1805.00500. URL: http://arxiv.org/abs/1805.00500.

[26] Jae-Hong Lee et al. “Detection and diagnosis of dental caries using a deep learning-based convolutional neural network algorithm”. In: *Journal of Dentistry* 77 (Oct. 2018), pp. 106–111. DOI: 10.1016/j.jdent.2018.07.015.

[27] Wook Joo Park and Jun-Beom Park. “History and application of artificial neural networks in dentistry”. In: *European journal of dentistry* 12.04 (2018), pp. 594–601.

[28] Mark Sandler et al. “Inverted Residuals and Linear Bottlenecks: Mobile Networks for Classification, Detection and Segmentation”. In: *CoRR* abs/1801.04381 (2018). arXiv: 1801.04381. URL: http://arxiv.org/abs/1801.04381.

[29] William W Stead. “Clinical implications and challenges of artificial intelligence and deep learning”. In: *Jama* 320.11 (2018), pp. 1107–1108.

[30] Xudong Sun, Pengcheng Wu, and Steven C.H. Hoi. "Face detection using deep learning: An improved faster RCNN approach". In: *Neurocomputing* 299 (2018), pp. 42–50. ISSN: 0925-2312. DOI: https://doi.org/10.1016/j.neucom.2018.03.030. URL: https://www.sciencedirect.com/science/article/pii/S0925231218303229.

[31] Qina Tian et al. "Pedestrian Detection Based on Laplace Operator Image Enhancement Algorithm and Faster R-CNN". In: *2018 11th International Congress on Image and Signal Processing, BioMedical Engineering and Informatics (CISP-BMEI)*. IEEE, Oct. 2018. DOI: 10.1109/cisp-bmei.2018.8633093.

[32] Giuseppe Carleo et al. "Machine learning and the physical sciences". In: *Reviews of Modern Physics* 91.4 (2019), p. 045002.

[33] Hu Chen et al. "A deep learning approach to automatic teeth detection and numbering based on object detection in dental periapical films". In: *Scientific Reports* 9.1 (Mar. 2019). DOI: 10.1038/s41598-019-40414-y.

[34] Dat Q. Duong et al. "Fully Automated Segmentation of Alveolar Bone Using Deep Convolutional Neural Networks from Intraoral Ultrasound Images". In: *2019 41st Annual International Conference of the IEEE Engineering in Medicine and Biology Society (EMBC)*. 2019, pp. 6632–6635. DOI: 10.1109/EMBC.2019.8857060.

[35] Jaeyoung Kim et al. "DeNTNet: Deep Neural Transfer Network for the detection of periodontal bone loss using panoramic dental radiographs". In: *Scientific Reports* 9.1 (Nov. 2019). DOI: 10.1038/s41598-019-53758-2.

[36] Joachim Krois et al. "Deep learning for the radiographic detection of periodontal bone loss". In: *Scientific reports* 9.1 (2019), pp. 1–6.

[37] Wen Li et al. "A gingivitis identification method based on contrast-limited adaptive histogram equalization, gray-level co-occurrence matrix, and extreme learning machine". In: *International Journal of Imaging Systems and Technology* 29.1 (2019), pp. 77–82.

[38] K. Moutselos et al. "Recognizing Occlusal Caries in Dental Intraoral Images Using Deep Learning". In: *2019 41st Annual International Conference of the IEEE Engineering in Medicine and Biology Society (EMBC)*. IEEE, July 2019. DOI: 10.1109/embc.2019.8856553.

[39] Muhammad Sajad, Imran Shafi, and Jamil Ahmad. "Automatic Lesion Detection in Periapical X-rays". In: *2019 International Conference on Electrical, Communication, and Computer Engineering (ICECCE)*. IEEE, July 2019. DOI: 10.1109/icecce47252.2019.8940661.

[40] Toufique Ahmed Soomro et al. "Impact of Image Enhancement Technique on CNN Model for Retinal Blood Vessels Segmentation". In: *IEEE Access* 7 (2019), pp. 158183–158197. DOI: 10.1109/access.2019.2950228.

[41] Anselmo Garcia Cantu et al. "Detecting caries lesions of different radiographic extension on bitewings using deep learning". In: *Journal of Dentistry* 100 (Sept. 2020), p. 103425. DOI: 10.1016/j.jdent.2020.103425.

[42] V Geetha, KS Aprameya, and Dharam M Hinduja. "Dental caries diagnosis in digital radiographs using back-propagation neural network". In: *Health Information Science and Systems* 8.1 (2020), pp. 1–14.

[43] Anuradha Laishram and Khelchandra Thongam. "Detection and Classification of Dental Pathologies using Faster-RCNN in Orthopantomogram Radiography Image". In: *2020 7th International Conference on Signal Processing and Integrated Networks (SPIN)*. IEEE, Feb. 2020. DOI: 10.1109/spin48934.2020.9071242.

[44] Jae-Hong Lee, Do-Hyung Kim, and Seong-Nyum Jeong. "Diagnosis of cystic lesions using panoramic and cone beam computed tomographic images based on deep learning neural network". In: *Oral diseases* 26.1 (2020), pp. 152–158.

[45] Ki-Sun Lee et al. "Deep Convolutional Neural Networks Based Analysis of Cephalometric Radiographs for Differential Diagnosis of Orthognathic Surgery Indications". In: *Applied Sciences* 10.6 (2020). ISSN: 2076-3417. DOI: 10.3390/app10062124. URL: https://www.mdpi.com/2076-3417/10/6/2124.

[46] Haoyang Li et al. "Automatic and interpretable model for periodontitis diagnosis in panoramic radiographs". In: June 2020.

[47] Maira Beatriz Hernandez Moran et al. "On using convolutional neural networks to classify periodontal bone destruction in periapical radiographs". In: *2020 IEEE International Conference on Bioinformatics and Biomedicine (BIBM)*. IEEE. 2020, pp. 2036–2039.

[48] K.C.T. Nguyen et al. “Alveolar Bone Segmentation in Intraoral Ultrasonographs with Machine Learning”. In: *Journal of Dental Research* 99.9 (May 2020), pp. 1054–1061. DOI: 10.1177/0022034520920593.

[49] Siti Fairuz Mat Radzi et al. “Impact of Image Contrast Enhancement on Stability of Radiomics Feature Quantification on a 2D Mammogram Radiograph”. In: *IEEE Access* 8 (2020), pp. 127720–127731. DOI: 10.1109/access.2020.3008927.

[50] Zhiyang Zheng et al. “Anatomically constrained deep learning for automating dental CBCT segmentation and lesion detection”. In: *IEEE Transactions on Automation Science and Engineering* 18.2 (2020), pp. 603–614.

[51] Nabeel Khalid et al. “DeepCeNS: An end-to-end Pipeline for Cell and Nucleus Segmentation in Microscopic Images”. In: *2021 International Joint Conference on Neural Networks (IJCNN)*. IEEE, July 2021. DOI: 10.1109/ijcnn52387.2021.9533624.

[52] Hassan Aqeel Khan et al. “Automated feature detection in dental periapical radiographs by using deep learning”. In: *Oral Surgery, Oral Medicine, Oral Pathology and Oral Radiology* 131.6 (June 2021), pp. 711–720. DOI: 10.1016/j.oooo.2020.08.024.

[53] Shammi Kolonne et al. “MobileNetV2 Based Chest X-Rays Classification”. In: *2021 International Conference on Decision Aid Sciences and Application (DASA)*. IEEE, Dec. 2021. DOI: 10.1109/dasa53625.2021.9682248.

[54] Md Mijanur Rahman et al. “A Comprehensive Study of Artificial Intelligence and Machine Learning Approaches in Confronting the Coronavirus (COVID-19) Pandemic”. In: *International Journal of Health Services* 51.4 (May 2021), pp. 446–461. DOI: 10.1177/00207314211017469.

[55] Xiaoyong Yang et al. “Colon Polyp Detection and Segmentation Based on Improved MRCNN”. In: *IEEE Transactions on Instrumentation and Measurement* 70 (2021), pp. 1–10. DOI: 10.1109/tim.2020.3038011.

[56] A. Ramana Kumari, Suryakari Nagaraja Rao, and P. Ramana Reddy. “Design of hybrid dental caries segmentation and caries detection with meta-heuristic-based ResneXt-RNN”. In: *Biomedical Signal Processing and Control* 78 (Sept. 2022), p. 103961. DOI: 10.1016/j.bspc.2022.103961.

[57] Chun-Teh Lee et al. “Use of the deep learning approach to measure alveolar bone level”. In: *Journal of clinical periodontology* 49.3 (2022), pp. 260–269.

[58] Shuai Li et al. “Automatic Dental Plaque Segmentation Based on Local-to-Global Features Fused Self-Attention Network”. In: *IEEE Journal of Biomedical and Health Informatics* 26.5 (2022), pp. 2240–2251.

[59] Karen Panetta et al. “Tufts Dental Database: A Multimodal Panoramic X-Ray Dataset for Benchmarking Diagnostic Systems”. In: *IEEE Journal of Biomedical and Health Informatics* 26.4 (Apr. 2022), pp. 1650–1659. DOI: 10.1109/jbhi.2021.3117575.

[60] Jinyoung Park and Hoseok Moon. “Lightweight Mask RCNN for Warship Detection and Segmentation”. In: *IEEE Access* 10 (2022), pp. 24936–24944. DOI: 10.1109/ACCESS.2022.3149297.

[61] Umer Rashid et al. “A hybrid mask RCNN-based tool to localize dental cavities from real-time mixed photographic images”. In: *PeerJ Computer Science* 8 (Feb. 2022), e888. DOI: 10.7717/peerj-cs.888.

[62] Gurpreet Kour Sodhi et al. “COVID-19: Role of Robotics, Artificial Intelligence and Machine Learning During the Pandemic”. In: *Current Medical Imaging Formerly Current Medical Imaging Reviews* 18.2 (Feb. 2022), pp. 124–134. DOI: 10.2174/1573405617666210224115722.

[63] Yuang Zhu et al. “Faster-RCNN based intelligent detection and localization of dental caries”. In: *Displays* 74 (Sept. 2022), p. 102201. DOI: 10.1016/j.displa.2022.102201.

[64] *Artificial Intelligence in Medicine | IBM*. https://www.ibm.com/topics/artificial-intelligence-medicine/. Accessed: 2022-08-25.

[65] Abhishek Dutta. *VGG Image annotator*. URL: https://annotate.officialstatistics.org/.

[66] *Mean average precision (MAP) explained: Everything you need to know*. URL: https://www.v7labs.com/blog/mean-average-precision.

[67] *Mobilenetv2: The next generation of on-device computer vision networks*. https://ai.googleblog.com/2018/04/mobilenetv2-next-generation-of-on.html/. Accessed: 2022-08-25.

[68] S.M. Pizer et al. “Contrast-limited adaptive histogram equalization: speed and effectiveness”. In: *[1990] Proceedings of the First Conference on Visualization in Biomedical Computing*. IEEE Comput. Soc. Press. DOI: 10.1109/vbc.1990.109340.

[69] *Understanding Mask R-CNN Basic Architecture*. https://www.shuffleai.blog/blog/Understanding_Mask_R-CNN_Basic_Architecture.html. Accessed: 2022-08-28.